International Journal of Pharmaceutics 426 (2012) 271–279

Contents lists available at SciVerse ScienceDirect

International Journal of Pharmaceutics

journal homepage: www.elsevier.com/locate/ijpharm

Pharmaceutical Nanotechnology

Hemocompatibility of poly(ε-caprolactone) lipid-core nanocapsules stabilized with polysorbate 80-lecithin and uncoated or coated with chitosan

Eduardo A. Bender[a], Márcia D. Adorne[c], Letícia M. Colomé[a], Dulcinéia S.P. Abdalla[b], Sílvia S. Guterres[a,d], Adriana R. Pohlmann[a,c,d,*]

[a] Programa de Pós-Graduação em Ciências Farmacêuticas, Faculdade de Farmácia, Universidade Federal do Rio Grande do Sul, Av. Ipiranga, 2752, Porto Alegre, 90610-000, RS, Brazil
[b] Faculdade de Ciências Farmacêuticas, Universidade de São Paulo, Av. Professor Lineu Prestes, 580, bloco 17, São Paulo, 05508-900, SP, Brazil
[c] Departamento de Química Orgânica, Instituto de Química, Universidade Federal do Rio Grande do Sul, PBox 15003, Porto Alegre, 91501-970, RS, Brazil
[d] Centro de Nanociência e Nanotecnologia, CNANO-UFRGS, Universidade Federal do Rio Grande do Sul, Av. Bento Gonçalves, 9500, Porto Alegre, 91501-970, RS, Brazil

ARTICLE INFO

Article history:
Received 5 September 2011
Received in revised form 19 January 2012
Accepted 24 January 2012
Available online 1 February 2012

Keywords:
Hemocompatibility
Polymeric nanoparticles
Lipid-core nanocapsules
Polysorbate 80
Lecithin
Chitosan

ABSTRACT

The hemocompatibility of nanoparticles is of critical importance for their systemic administration as drug delivery systems. Formulations of lipid-core nanocapsules, stabilized with polysorbate 80-lecithin and uncoated or coated with chitosan (LNC and LNC-CS), were prepared and characterized by laser diffraction (*D*[4,3]: 129 and 134 nm), dynamic light scattering (119 nm and 133 nm), nanoparticle tracking (D50: 124 and 139 nm) and particle mobility (zeta potential: −15.1 mV and +9.3 mV) analysis. In vitro hemocompatibility studies were carried out with mixtures of nanocapsule suspensions in human blood at 2% and 10% (v/v). The prothrombin time showed no significant change independently of the nanocapsule surface potential or its concentration in plasma. Regarding the activated partial thromboplastin time, both suspensions at 2% (v/v) in plasma did not influence the clotting time. Even though suspensions at 10% (v/v) in plasma decreased the clotting times ($p < 0.05$), the values were within the normal range. The ability of plasma to activate the coagulation system was maintained after the addition of the formulations. Suspensions at 2% (v/v) in blood showed no significant hemolysis or platelet aggregation. In conclusion, the lipid-core nanocapsules uncoated or coated with chitosan are hemocompatible representing a potential innovative nanotechnological formulation for intravenous administration.

1. Introduction

Currently, research involving nanoparticulate systems applied to medicine has assumed a significant role in the obtainment of new and/or enhanced diagnostic and therapeutic methods for use in health promotion. In this context, most of these new technologies are intended for systemic use and thus their biocompatibility is an important issue (Koziara et al., 2005; Cenni et al., 2008; Michanetzis et al., 2008). Nanoparticles have been administered by systemic route mainly as platforms or carries for otherwise insoluble or poorly soluble drugs, imaging agents and gene delivery purposes (Dobrovolskaia et al., 2009). Among the applications, studies involving nanoparticles as agents for drug delivery in cancer therapy are highlighted (Byrne et al., 2008; Huynh et al., 2009). The main benefits of using nanoparticles as drug carriers include the reduction of side effects and the improvement of efficacy due to active or passive targeting of the carried drug to locations in the body where it can be most effective (Dobrovolskaia et al., 2009).

Despite the significant scientific interest and promising potential, the safety of nanoparticulate systems remains a growing concern considering that biological applications of nanoparticles could lead to unpredictable effects (Nafee et al., 2009; Zern et al., 2011). Ideal systems are those that prevent or delay protein adsorption onto the nanoparticle surface (opsonization), and their subsequent uptake by macrophages, prolonging the circulation time of the nanoparticles (Cai et al., 2009). Given their nanoscale size, nanoparticles might have a low hemocompatibility in comparison with their starting bulk materials due to the higher surface/volume ratio and the greater number of reactive groups on the surface (Cenni et al., 2008). Nanoparticles should neither activate platelets, hemolysis, coagulation factors, or signaling molecules for leukocytes nor induce damage to endothelial cells. These events are related to the occurrence of thrombotic, hemorrhagic, hemolytic and inflammatory events (Koziara et al., 2005; Mayer et al., 2009).

To avoid these events, one of the main goals in nanomedicine is to find biocompatible and biodegradable materials to obtain nanoparticulate systems. The most common choices are

* Corresponding author at: Instituto de Química, Universidade Federal do Rio Grande do Sul, CP 15003, Porto Alegre 91501-970, RS, Brazil. Tel.: +55 51 33087237; fax: +55 51 33087304.
E-mail address: pohlmann@iq.ufrgs.br (A.R. Pohlmann).

0378-5173/$ – see front matter © 2012 Elsevier B.V. All rights reserved.
doi:10.1016/j.ijpharm.2012.01.051

biodegradable and biocompatible polyesters such as poly(D,L-lactic acid) (PLA) (Jones and Grainger, 2009), poly(caprolactone) (PCL) (Cai et al., 2009) or poly(lactide-*co*-glycolide) (PLGA) (Nafee et al., 2009). Polymeric nanoparticles may also be coated with hydrophilic polymers, such as poly(ethylene glycol) (PEG) and methoxy poly(ethylene glycol), to reduce adsorption of the plasma proteins such as opsonins and apolipoproteins on their surface (Letchford et al., 2009; Byrne et al., 2008).

Similarly, polysorbate 80 [poly(oxyethylene)-sorbitan-20-monooleate] can be used to delay opsonization. Lipid-core nanocapsules stabilized with polysorbate 80 showed efficient delivery of drugs to the brain (Frozza et al., 2010) and to inflamed tissues (Bernardi et al., 2009). Furthermore, attempts have been made to modify the surface of PCL or PLGA nanoparticles using cationic polymers, such as chitosan (Cai et al., 2009; Nafee et al., 2009). Chitosan is a cationic polysaccharide with biocompatible and nontoxic properties making this polymer a good candidate for pharmaceutical applications (Oyarzun-Ampuero et al., 2010; Xu et al., 2010). Its hydrophilic nature and the presence of primary amine groups enable the association of delicate compounds such as peptides and proteins (Aktas et al., 2005; Baldrick, 2010). Chitosan nanoparticles have been used for widespread applications such as drug delivery, muco-adhesive dosage forms, rapid release forms, improved peptide delivery, colonic drug delivery and gene delivery (Cui and Mumper, 2001; Aktas et al., 2005; Wang et al., 2011). In addition, the use of chitosan-based nanoparticles as a nanoscale vaccine delivery system for subunit antigens has been proposed (Prego et al., 2010) as a new system for hepatitis B immunization.

Nanoparticles with cationic shells have been found to be toxic and it has been suggested that this toxicity is due to charge interactions with the plasma membrane and/or with negatively-charged cell components and proteins (Skotak et al., 2008; Nafee et al., 2009; Baldrick, 2010). On the other hand, negatively-charged nanoparticles can induce platelet aggregation to a greater extent than cationic or neutral nanoparticles (Koziara et al., 2005). Moreover, the ability of the nanoparticles to inhibit platelet aggregation is dependent on their particle size, as well as surface hydrophobicity and charge (Koziara et al., 2005; Xu et al., 2010).

Lipid-core nanocapsules, which are non-ionic carriers, have shown great potential as drug delivery systems for topical, oral or systemic applications (Alves et al., 2007; Cattani et al., 2010; Cruz et al., 2006; Bernardi et al., 2009; Frozza et al., 2010). The supramolecular structure of these new carriers has been fully investigated demonstrating that the core is composed of a dispersion of oil and sorbitan monostearate surrounded by the poly(ε-caprolactone) wall and stabilized by polysorbate 80 (Cruz et al., 2006; Jager et al., 2007, 2009).

Taking all of the above considerations into account, the objective of our study was to develop modified lipid-core nanocapsules by stabilizing them simultaneously with polysorbate 80 and lecithin to generate negatively-charged lipid-core nanocapsules, followed by coating with chitosan to obtain positively-charged lipid-core nanocapsules. Furthermore, we aimed to determine the hemocompatibility of both negatively and positively-charged formulations, herein referred to as LNC and LNC-CS, by evaluating their in vitro hemocompatibility with special focus on hemolytic activity, platelet function, membrane integrity, and blood coagulation.

2. Material and methods

2.1. Materials

Poly(ε-caprolactone) (PCL) (α,ω-dihydroxy functional polymer; Mn 10,000 g mol^{-1}, Mw 14,000 g mol^{-1}), low molar weight chitosan (Mw 50,000–190,000 g mol^{-1}, 75–85% deacetylated polymer), sorbitan monostearate (Span 60®) and Triton X-100 were supplied by Sigma–Aldrich (U.S.). Lipoid S75 (soybean lecithin) was obtained from Lipoid (Germany). Caprylic/capric triglyceride and polysorbate 80 were purchased from Delaware (Brazil). Reagent kits to measure prothrombin time (PT) and activated partial thromboplastin time (APTT), for hemoglobin analysis and for the determination of the activity of enzyme lactate dehydrogenase (LDH) and commercial standard serum (Qualitrol 1H) were purchased from Labtest Diagnóstica (Brazil). All aqueous solutions were prepared with deionized water (DI) using a Millipore Direct-Q system with a resistivity of 18.2 MΩ. The solvents, acetone and ethanol PA, were obtained from Nuclear (Brazil). PBS buffer (pH 7.2), May–Grünwald and Giemsa stains, EDTA K_2 and sodium citrate anticoagulants were obtained from Laborclin (Brazil). All reagents were used as received.

2.2. Preparation of lipid-core nanocapsule aqueous suspensions

A formulation of lipid-core nanocapsules stabilized with polysorbate 80 and lecithin was prepared using a methodology previously reported for lipid-core nanocapsules stabilized with polysorbate 80 (Jager et al., 2009). The methodology is based on the principle of interfacial deposition of pre-formed polymers reported for polymeric nanocapsules (Fessi et al., 1989).

The procedure consisted of an organic phase containing PCL (0.1 g), sorbitan monostearate (0.04 g), and caprylic/capric triglyceride (0.12 g) dissolved in acetone (25 mL). In parallel, an ethanolic solution (5 mL) containing lecithin (0.03 g) was prepared and poured into the organic phase. This mixture was then poured into an aqueous solution (50 mL) containing polysorbate 80 (0.08 g) under moderate magnetic stirring at 40 °C. After 10 min, the mixture was evaporated under reduced pressure to eliminate the acetone and to concentrate the suspension (near 9 mL). The final volume was adjusted in a volumetric flask to 10 mL. This formulation was called LNC.

To coat the lipid-core nanocapsules, a 0.3% (w/v) chitosan solution was prepared by dissolving the polysaccharide in 10 mL of 1% acetic acid aqueous solution. This solution (1 mL) was slowly added to 9 mL of LNC suspension under moderate magnetic stirring. The reaction medium remained under stirring for 4 h at room temperature. This formulation was called LNC-CS.

2.3. Physico-chemical characterization

2.3.1. Zeta potential

Zeta potential (ζ) was determined on a ZetaSizer Nano ZS (Malvern Instruments Ltd., UK). This equipment operates in the range of 3.8 nm to 100 μm. Measurements were taken at 25 °C. The samples were diluted (500×) in 10 mmol L^{-1} NaCl aqueous solution. To avoid any sample selection the formulations were added into pre-filtered medium without treatment (centrifugation or filtration). All samples were analyzed in triplicate batches (n = 3).

2.3.2. pH measurements

The pH of the lipid-core nanocapsule suspensions was measured without previous dilution using a calibrated potentiometer B474 (Micronal, Brazil) at 25 °C. All samples were analyzed in triplicate batches (n = 3).

2.3.3. Granulometric profiles and mean diameters by laser diffraction

The size distribution profiles were determined by laser diffraction using a Mastersizer 2000 (Malvern Instruments Ltd., UK). This equipment measures materials in the range of 0.02–2000 μm. Each sample was directly inserted into the wet sample dispersion unit without previous treatment. Mean particle diameters were

described as volume-weighted mean diameters ($D_{4,3}$). All samples were analyzed in triplicate batches ($n = 3$).

2.3.4. Particle sizing by dynamic light scattering

The formulations were also characterized by dynamic light scattering (DLS) using a ZetaSizer Nano ZS (Malvern Instruments Ltd., UK). This equipment operates in a working size range of 0.3 nm to 10.0 μm. The measurements were taken at 25 °C. The average diameters were determined after diluting the samples (500×) in ultrapure water. To avoid any sample selection the formulations were added into pre-filtered medium without treatment (centrifugation or filtration). All samples were analyzed in triplicate batches ($n = 3$).

2.3.5. Nanoparticle tracking analysis

Nanoparticle tracking analysis (NTA) is a method of visualizing and analyzing particles in liquid dispersions (NanoSight LM10 & NTA 2.0 Analytical Software, NanoSight Ltd.). This technique measures particles in the range of 10–1000 nm. NTA is carried out using a small amount of the diluted samples (0.5 mL) introduced into the chamber by a syringe. The chamber is placed on an optical microscope and the particles are illuminated by a laser diode (635 nm wavelength). The video images of the Brownian motion of the individual particles are followed in real-time via CCD camera and analyzed using the NTA 2.0 Analytical Software (NanoSight®).

The light scattered by the particles is captured by a digital camera and the motion of each particle is tracked from frame to frame. The rate of particle movement is related to a sphere equivalent hydrodynamic radius as calculated using the Stokes–Einstein equation. The particle size distributions are calculated on a particle by particle basis. Visible particles in the frame correspond to each separate light scattering center which is seen as an individual particle during filming (Filipe et al., 2010).

The formulations were diluted 5000 times using ultrapure water (MillQ®) and each video clip was captured over 120 s. The automatic detection threshold was enabled and the maximum particle jump was set at 10 in the NTA software. All measurements were performed in triplicate batches. The polydispersity of the particle sizes was calculated as *Span*, which is the width of the distribution based on the 10%, 50% and 90% of the cumulative distribution of sizes.

2.3.6. Multiple light scattering

To check the colloidal physical stability, the lipid-core nanocapsule suspensions were evaluated by multiple light scattering using a Turbiscan LA*b* (Formulaction, France). In this method the light source is an electro luminescent diode in the near infrared (880 nm wavelength) and two synchronous optical sensors receive, respectively, the light transmitted through the sample (0° from the incident light, transmission sensor), and the light backscattered by the sample (135° from the incident radiation, backscattering detector), acquiring transmission and backscattering data every 40 μm from the bottom to the top of the cell (Mengual et al., 1999). The samples (10 mL) were poured into the glass cells without any treatment or dilution and analyzed at 25 °C for 1 h using the scan mode.

2.4. Blood compatibility

2.4.1. Blood and plasma samples

Whole blood was collected from a healthy human volunteer in an evacuated siliconized glass tube containing 3.2% sodium citrate or EDTA as anticoagulants. All blood samples were obtained from the *Faculdade de Farmácia* at the *Universidade Federal do Rio Grande do Sul* (Brazil). As the stages of blood collection and centrifugation are critical to the platelet activation status, the blood samples were obtained without tourniquet. Ethical approval for this study was granted by the Human Ethics Committee of the *Universidade Federal do Rio Grande do Sul*, Brazil (protocol # 19404, UFRGS).

2.4.2. Plasma clotting

Platelet-poor plasma was prepared by centrifugation of freshly drawn whole blood for 10 min, at 1344 × *g* and either used fresh or stored at −20 °C. The APTT and PT were determined by the appearance of a macroscopic clot which indicated the end of the reaction. Lipid-core nanocapsule suspensions (LNC and LNC-CS) were added to the plasma samples at 2 and 10% (v/v) and stirred for 1 h at 37 °C. For the PT determination, PT Hemostasis reagent (Labtest®) was added to the sample, whereas for APTT partial thromboplastin reagent (Labtest®) was added along with calcium chloride. Normal controls consisted of equivalent volumes of PBS added to the plasma at the same concentrations used for the nanocapsule suspensions. All experiments were performed at 37 °C and in triplicate batches ($n = 3$).

2.4.3. Hemolysis

Hemolysis induced by particle treatment was assessed photometrically with a colorimetric endpoint hemoglobin reagent kit (Labtest®). Whole blood was collected in an evacuated siliconized glass tube containing EDTA as an anticoagulant and the number of erythrocytes present (4.76×10^6 cells μL^{-1}) was determined using an automated hematology counter (ABX Micros 60, Horiba-ABX, France). Formulations (LNC and LNC-CS) were incubated at 2 and 10% (v/v) with the whole blood at 37 °C. A spontaneous hemolysis control was prepared by incubating erythrocytes with PBS, also at 2 and 10% (v/v). A 100% hemolysis control was prepared by incubating erythrocytes with an equal volume of Triton X-100 (1%). As the internal quality control, we used a commercial standard of hemoglobin produced by the manufacturer of the hemoglobin kit. All tubes were incubated at 37 °C with tumbling. At time intervals of 1, 2, 4 and 8 h the tubes were centrifuged at 1344 × *g* for 10 min and the hemoglobin released into the supernatant was detected at 540 nm (UV-Vis 1601 PC Spectrophotometer, Schimadzu, Japan). The percentage of hemolysis was calculated for each sample (Eq. (1)).

$$\%Hemolysis = \frac{Abs_{sample} - Abs_{spontaneous}}{Abs_{100\%\,hemolysis}} \times 100 \quad (1)$$

where Abs_{sample} is the absorbance of the supernatant of erythrocytes incubated with nanoparticle suspension, $Abs_{spontaneous}$ is the absorbance of the supernatant of erythrocytes incubated with PBS suspension and, finally, $Abs_{100\%\,hemolysis}$ is the absorbance of the supernatant of the erythrocyte incubated with Triton X-100 (1%) solution in PBS suspension. All sample were analyzed in triplicate batches ($n = 3$).

2.4.4. Evaluation of the erythrocyte membrane integrity

The activity of the enzyme LDH released from erythrocytes by particle treatment was assessed photometrically using the LDH commercial kit (Labtest®). Firstly, for the removal of plasma and leukocytes, the erythrocyte concentrate was centrifuged for 10 min, at 1344 × *g* and room temperature. The peripheral blood mononuclear cells and plasma band were drawn with a Pasteur pipette. The pellet consisting of erythrocytes was washed three times with PBS. A 20% suspension of erythrocytes (9.52×10^5 cells μL^{-1} determined by ABX Micros 60, Horiba-ABX, France) in PBS was used for the experiments. Lipid-core nanocapsule suspensions (LNC and LNC-CS) were incubated at 2 and 10% (v/v) with the erythrocyte suspension at 37 °C. A spontaneous LDH control was prepared by incubation of the erythrocyte suspension with PBS, also at 2 and 10% (v/v). A 100% LDH control was prepared by the addition of an equal volume of erythrocyte suspension and Triton X-100 (1%). As the internal quality control, we used a commercial standard serum

(Qualitrol 1H – Labtest®). All tubes were incubated at 37 °C and stirred for 1 h. After that, the tubes were centrifuged at 1344 × *g* for 10 min and the LDH released in the supernatant was detected at 500 nm (UV-Vis 1601 PC Spectrophotometer, Schimadzu, Japan). The concentration of LDH released was calculated through Eq. (2).

$$Lactate\ \ dehydrogenase(\mathrm{U\ L^{-1}}) = \frac{Abs_{sample} - Abs_{control}}{Abs_{st}} \times 150 \quad (2)$$

where Abs_{sample} is the absorbance of the supernatant of the erythrocyte with nanoparticle suspension, $Abs_{control}$ is the absorbance of the supernatant of the erythrocyte without nanoparticle suspension added in the substrate reaction and finally, Abs_{st} is the absorbance of the supernatant of the erythrocyte with LDH standard (150 U L^{-1}, according to the manufacturer). All samples were analyzed in triplicate batches ($n = 3$).

2.4.5. Platelet aggregation tests

To identify platelet changes due to the particle treatment, peripheral blood smears were firstly prepared after the incubation of citrated whole blood with lipid-core nanocapsules. In brief, the samples were incubated with whole blood at 2 and 10% (v/v) for 30 min at 37 °C with gentle agitation (400 rpm). Likewise, in the same ratio, equal volumes of whole blood and PBS were incubated and served as the control of spontaneous platelet aggregation.

After incubation peripheral blood smears were stained, firstly for 3 min with May–Grünwald staining and secondly with Giensa staining for 15 min (Bioclin, Brazil). After rinsing in water the dried smears were analyzed with an optical microscope (Primo Star, Zeiss, Germany) in immersion objective and images were collected using the digital system (Canon PC 1250 and Soligor adapter tube for Canon A 650 IS B52 wide, Japan).

In a second step we evaluated platelet aggregation in citrated whole blood samples before and after addition of LNC and LNC-CS at 2 and 10% (v/v). The citrated whole blood containing nanoparticle suspensions remained under gentle agitation (400 rpm) for 30 min at 37 °C before analysis. We used a hematological counter (ABX Micros 60, Horiba-ABX, France) that determined by laser diffraction the platelet count and established the mean platelet volume (MPV). All samples were analyzed in triplicate batches ($n = 3$).

2.5. Statistical analysis

All results are expressed as the mean value ± the standard deviation of the mean and were statistically analyzed using analysis of variance (ANOVA). Results presenting $p < 0.05$ were considered statistically different. The comparisons among the averages were performed using Tukey's test.

3. Results and discussion

3.1. Preparation of lipid-core nanocapsules

Negatively-charged lipid-core nanocapsules (LNC) were prepared by interfacial deposition of polymer using sorbitan monostearate and caprilic/capric triglyceride as the lipid dispersion in the core, poly(ε-caprolactone) as the polymer wall, and polysorbate 80 and lecithin as stabilizers. Chitosan was used as the coating material for a second formulation in order to evaluate the influence of the surface charge on the hemocompatibility properties of the lipid-core nanocapsules. In this case, chitosan-coated lipid core nanocapsules (LNC-CS) were obtained after adding a chitosan solution to a sample of LNC. Both formulations had a white-bluish opalescent aspect with the Tyndall effect.

The LNC showed a negative zeta potential of −15.1 ± 1.0 mV, while LNC-CS had a positive value of +9.3 ± 2.5 mV. The zeta potential determined for LNC is slightly more negative than the value observed for lipid-core nanocapsules prepared without lecithin (−9.4 ± 0.7 mV) (Jager et al., 2009). According to the literature (Mosqueira et al., 2000), the presence of phosphatidic acid, as an impurity in lecithin, is responsible for the negative charge on the particle surface. The positive zeta potential value observed for LNC-CS indicated that chitosan is located at the particle–water interface, externally coating the lipid-core nanocapsules.

The lipid-core nanocapsule suspensions showed pH values of 5.2 ± 0.1 for LNC and 3.8 ± 0.2 for LNC-CS. The more pronounced acidity after coating with chitosan is a consequence of the 1% acetic acid aqueous solution used to dissolve the polysaccharide.

3.2. Granulometry and particle sizing

The laser diffraction technique was used to determine the granulometric profiles of the formulations. Since the suspensions are directly inserted into the sample dispersing unit this analysis is able to determine the purity of the submicrometric population and their size distribution profiles demonstrating the homogeneity of the nanoparticle population.

The granulometric profiles (by volume) showed unimodal size distributions for LNC and LNC-CS suspensions (Fig. 1A and C). The volume-weighted mean diameters ($D_{4,3}$) were 129 nm (LNC) and 134 nm (LNC-CS). The results indicated that no microscopic contamination is present in the formulations. It is noteworthy that the measurements were carried out by placing each sample directly into the wet sample dispersion unit without previous treatment (filtration or centrifugation). Thus, the preparation process produced quantitative yields of particles in the submicrometric range. Furthermore, the LNC coating did not cause any precipitation or agglomeration. Besides a slight broadening of the size distributions, the lipid-core nanocapsules maintained their nanometric sizes after coating with chitosan.

Moreover, the size distributions plotted by number (Fig. 1B and D) showed almost superposed profiles compared to the distributions by volume (Fig. 1A and C). The results indicated that both formulations present high homogeneity of nanoscopic populations, and verified narrow size distributions for both colloidal suspensions (LNC and LNC-CS).

LNC and LNC-CS were considered suitable formulations for follow-up studies, since they are composed of self-assembled biocompatible materials presenting particle sizes lower than 500 nm. These characteristics are of great importance when parenteral administration is the goal for therapeutic applications.

To characterize the hydrodynamic diameters of the LNC and LNC-CS suspensions, DLS and NTA were performed. The DLS analysis indicated that the particles had *z*-average diameters of 119 ± 1.71 nm and 133 ± 1.72 nm and polydispersity indexes lower than 0.17 (Table 1). The size distribution profiles showed unimodal populations by intensity, volume or number (data not shown). The data indicated a high degree of homogeneity in the particle size of the nanometric population in each sample.

Considering the NTA analysis, Brownian motion of the nanocapsules in suspension was observed by registering the light scattered. Well dispersed and spatially resolved particles were visualized in the frame images obtained from the random motion of the particles in suspension captured using a CCD camera for LNC (temperature 22.8 °C and viscosity 0.94 cP) and LNC-CS (temperature 22.6 °C and viscosity 0.94 cP). These images show a microscopic view of the scattering particles illuminated by the laser diode. Larger particles scatter more light and larger luminous dots appeared in the video frame, while smaller particles move faster and longer distances with respect to larger ones (Jakubowicz, 2008; Gallego-Urrea et al., 2009). Even though different intensities of light scattering can be observed for each formulation, cumulative data obtained for the percentile of the particle distribution by NTA showed diameters in

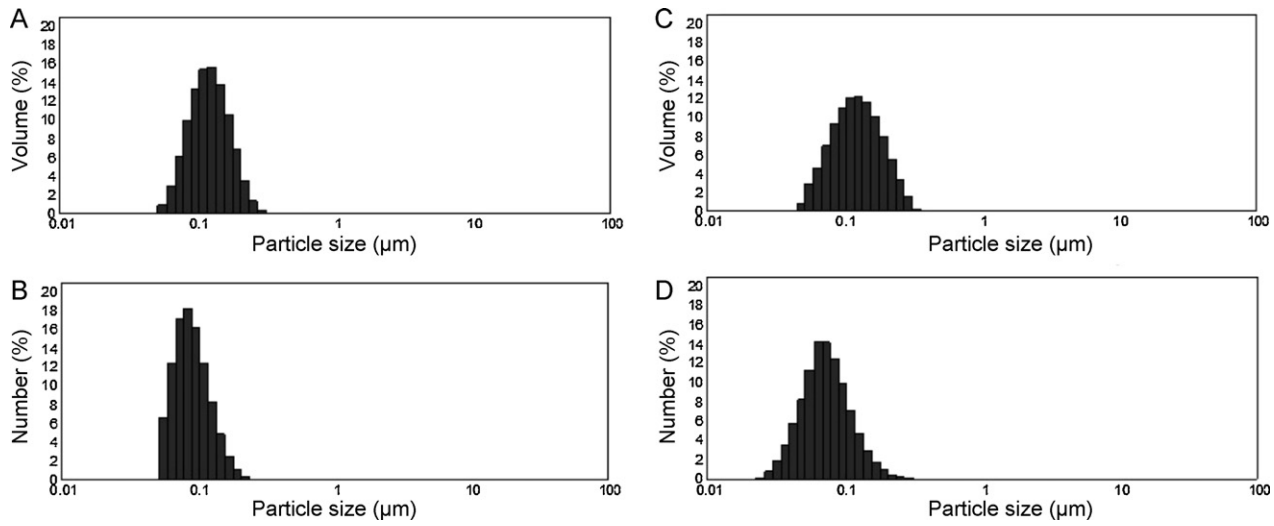

Fig. 1. Granulometric profiles obtained by laser diffraction for LNC (A and B) and LNC-CS (C and D). Parameters demonstrated by volume and number of particles ($n = 3$).

a narrow size distribution (Table 1). Furthermore, the polydispersity (Span) was lower than 1 (0.72 for LNC and 0.78 for LNC-CS) confirming the homogeneity and narrow size distribution of the LNC and LNC-CS. The different proportions of dilution for the DLS and NTA analyses did not influence the particle mean size.

Comparing DLS and NTA, similar sizes of particles for LNC and LNC-CS were determined. Thus, the data indicate that LNC were obtained in a narrow size distribution without the need for purification to yield exclusively one population of nanoscopic particles. In addition, the coating with chitosan did not modify the aggregation state of the LNC and did not cause agglomeration or precipitation in the suspension. Furthermore, LNC-CS had an average particle size 15 nm greater than LNC (Table 1). This change in the mean particle size observed after coating with chitosan and the inversion of the zeta potential maintaining a single population of particles, confirmed the high quality, homogeneity and reproducibility in obtaining and coating the lipid-core nanocapsules.

3.3. Physical stability determined by multiple light scattering

Multiple light scattering analysis by Turbiscan® can be used to determine reversible (creaming and sedimentation) and irreversible (coalescence and segregation) destabilization phenomena directly in the formulation without any prior dilution or treatment more easily than other techniques (Celia et al., 2009). LNC and LNC-CS are opaque and no transmission was detected by multiple light scattering analysis. Thus, variations in backscattering were analyzed.

Negative variations in the relative backscattering at the top of the cells were observed (−2% for LNC and −3% for LNC-CS). The small values determined during the experimental period indicated slow sedimentation. No variation at the middle of the cell was observed indicating the absence of flocculation or coalescence. LNC and LNC-CS presented density higher than the external phase as expected considering the density of the raw materials.

3.4. Blood hemocompatibility

3.4.1. Plasma clotting

The compatibility of the LNC and LNC-CS samples with human blood was evaluated by investigating their ability to alter the coagulation times and cause hemolysis. Coagulation of human blood was assessed in the presence of either LNC or LNC-CS suspensions at 2 and 10% (v/v) in citrated plasma samples (Fig. 2). The concentrations of lipid-core nanocapsule suspensions in plasma were chosen based on an acceptable volume for i.v. bolus administration (lower concentration, 2%, v/v) and on a large excess (higher concentration, 10%, v/v).

The blood coagulation cascade included intrinsic, extrinsic and common pathways. APTT and PT are mainly used to examine the intrinsic and extrinsic pathways, respectively (Letchford et al., 2009; Xu et al., 2010). In PT analysis, LNC (13.7 ± 0.3 s) and LNC-CS (14.4 ± 0.7 s), both at 2% (v/v) in plasma, caused no statistical difference in the clotting times compared to the 2% PBS control (12.9 ± 0.8 s). However, these formulations caused a significant increase in the clotting time compared to the 10% (v/v) PBS control group (13 ± 0.5 s) when the amount of suspension added to the plasma was 10% (v/v) (LNC 15 ± 0.8 s and LNC-CS 15.1 ± 1 s) ($p < 0.05$) (Fig. 2A).

The effects on the extrinsic pathway of blood coagulation are better evaluated when the measurement of time until fibrin clot formation are standardized in terms of percentage of prothrombin activity. At 2% (v/v) in the plasma, LNC and LNC-CS showed high prothrombin activity: 88% and 81%, respectively. Lower values for prothrombin activity were observed when the amount of suspension added to the plasma was 10% (v/v) (76% for LNC and 73% for LNC-CS). These results indicated that LNC and LNC-CS suspensions

Table 1
Average particle size and polydispersity index (PDI) determined by dynamic light scattering (DLS), D10, D50 and D90 diameters based on 10%, 50% and 90% of the cumulative distribution profile, and mean size determined by nanoparticle tracking analysis (NTA) for LNC and LNC-CS suspensions ($n = 3$).

Sample	Dynamic light scattering (DLS)		Nanoparticle tracking analysis (NTA)			
	z-Average diameter (nm)	PDI	Cumulative data			Mean (nm)
			D10 (nm)	D50 (nm)	D90 (nm)	
LNC	119 ± 1.71	0.10 ± 0.01	85	124	174	128 ± 35
LNC-CS	133 ± 1.12	0.17 ± 0.02	94	139	202	145 ± 46

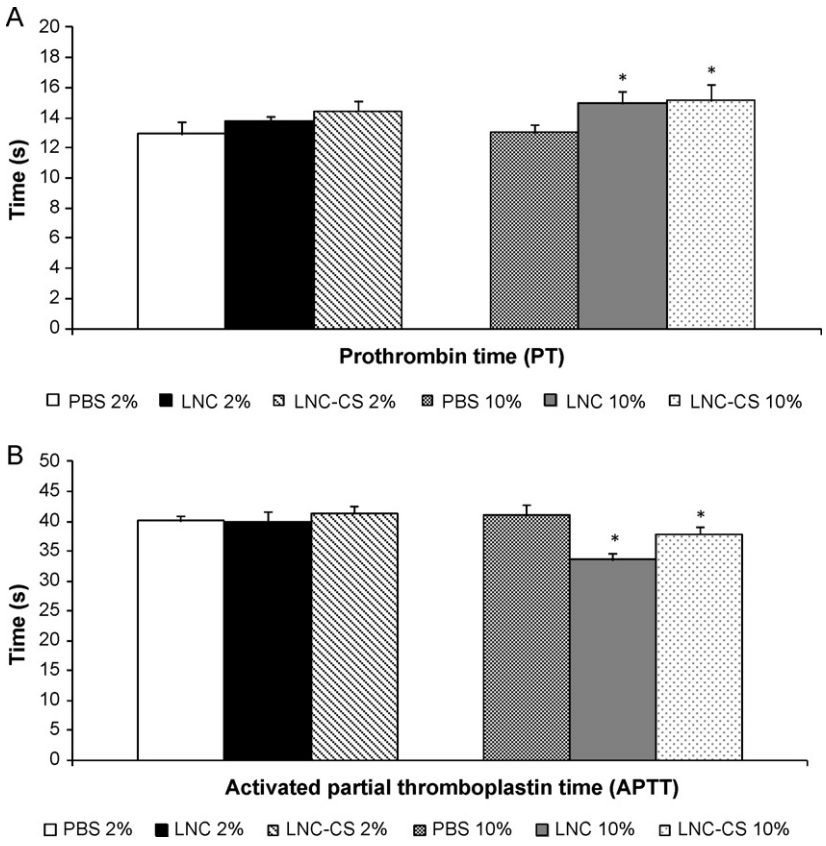

Fig. 2. Effect of lipid-core nanocapsules on the (A) prothrombin time (PT) and (B) activated partial thromboplastin time (APTT). LNC and LNC-CS in plasma at 2% and 10% (v/v) were compared to PBS controls. All bars represent mean clotting time ± SD ($n = 3$). *$p < 0.05$, different from control.

added at 2% (v/v) to the plasma did not influence the extrinsic pathway of blood coagulation maintaining the in vitro anticoagulation activity. Furthermore, even though a high concentration of lipid-core nanocapsules is added (10%, v/v) prothrombin activity levels are in a range greater that 70% (Cenni et al., 2008; von Ahsen et al., 2000).

Considering the intrinsic pathway of the blood coagulation cascade, the coagulation times obtained for the APTT analysis showed that LNC (39.9 ± 1.7 s) and LNC-CS (41.4 ± 1.2 s) suspensions at 2% (v/v) in plasma did not influence the clotting time compared to the 2% PBS (v/v) control (40 ± 0.8 s). However, when these lipid-core nanocapsule suspensions were added at 10% (v/v) in plasma, significant decreases in the clotting times were observed for LNC (33.5 ± 1.2 s) and LNC-CS (37.9 ± 1.2 s) compared to the 10% PBS (v/v) control (41 ± 1.7 s) ($p < 0.05$) (Fig. 2B). The reference ranges vary depending on the type of population studied; however, for guidance purposes, some authors report that the time until clot formation is usually between 32 and 46 s (Letchford et al., 2009). In this case, the decreases in plasma clotting times observed for LNC and LNC-CS at 10% (v/v) in plasma were considered to be of minor concern as the experimental values were within the normal range.

The results demonstrated that the ability of plasma samples to activate the coagulation system was maintained after the addition of lipid-core nanocapsule suspensions. Even using a concentration of 10% (v/v) of lipid-core nanocapsule suspensions in plasma, there was no impairment of the anticoagulant ability via the extrinsic or intrinsic pathway. Moreover, plasma coagulation factors were preserved in the presence of both formulations. At higher concentrations, the number of nanocapsules is high and the adsorption of coagulation factors could cause their deficiency in plasma promoting an increase in the time until the formation of a fibrin clot. Moreover, the coagulation profiles for LNC or LNC-CS ($p > 0.05$) did not differ when 10% (v/v) of nanocapsule suspension was added to the plasma.

3.4.2. Hemolysis

Another important feature in the development of nanoparticulate systems for parenteral administration is to determine their ability to cause hemolysis. Therefore, LNC and LNC-CS were evaluated for their ability to cause lysis in human erythrocytes (Fig. 3). Nanoparticulate systems should not favor the formation of hemolytic events when administered intravenously. In order to preserve the integrity and functionality of erythrocytes in whole blood samples, the limits prescribed by Brazilian law and

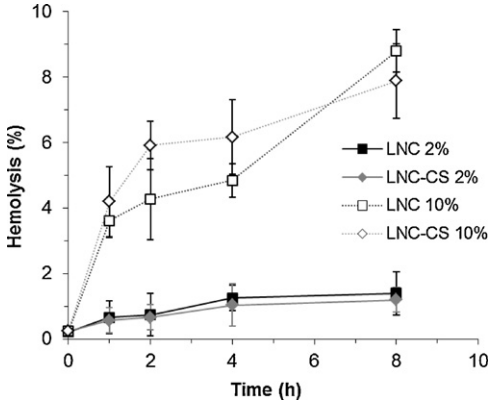

Fig. 3. Hemolysis assessed by release of hemoglobin in whole blood samples after the addition of LNC and LNC-CS suspensions to blood at 2% and 10% (v/v). All points represent mean hemolysis time ± SD ($n = 3$).

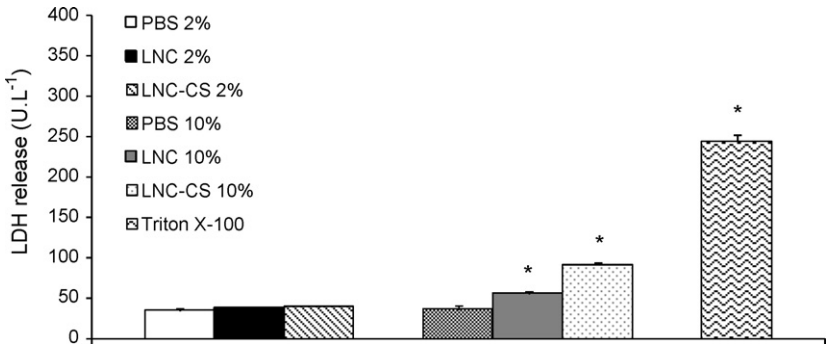

Fig. 4. Erythrocyte lactate dehydrogenase release (LDH) after treatment with LNC and LNC-CS suspensions. Triton X-100 (1%) was considered 100% of cell damage. All bars represent mean LDH release ± SD ($n = 3$). *$p < 0.05$, different from control.

international standards is 1% for spontaneous hemolysis (Hogman et al., 1981; Brazil, 2010).

In this study, the values of hemolysis remained restricted to the limits recommended when the whole blood was incubated with either LNC or LNC-CS suspensions at 2% (v/v) for 1, 2, 4 and 8 h of incubation. On the other hand, when the suspensions were added to blood at 10% (v/v), with the same period of incubation, hemoglobin was readily released into the extracellular environment, reaching the average rate of 8% at the end of 8 h of incubation. This result could be explained either by a shift in polysorbate 80 from the colloids to the cells or by the interaction of chitosan with the cells due to the high concentration used (10%, v/v) causing the hemolysis. As previously described, surfactant molecules can penetrate and saturate the membrane causing solubilization of the lipids and proteins (Jones, 1999; Letchford et al., 2009); and cationic polymers can cause injury to erythrocytes due to electrostatic interactions (Nafee et al., 2009). Thus, the high specific surface area of the colloids, when LNC and LNC-CS suspensions were added to blood at 10% (v/v), could explain the injury to the erythrocyte membrane.

3.4.3. Evaluation of the erythrocyte membrane integrity

The evaluation of the membrane integrity was also assessed by quantifying the enzyme LDH (Fig. 4). In this experiment the leukocytes and plasma were removed and only red blood cells in PBS were used to quantify the enzyme. This allowed the quantification of the erythrocyte LDH released and the evaluation of possible disturbances in membrane integrity.

LNC and LNC-CS at 2% (v/v) in blood did not cause a significant increase in erythrocyte LDH release when compared to the spontaneous release observed using PBS in the cell suspension after 30 min of incubation. The results indicated the maintenance of the membrane integrity in the presence of either LNC or LNC-CS at 2% (v/v) in blood. Thus, this reinforces the hypothesis that blood containing these lipid-core nanocapsules at this concentration may not damage the erythrocyte membrane to the point of releasing the hemoglobin component (complete rupture). Furthermore, the erythrocytes maintained their permeability, observed by assessing the LDH release. On the other hand, when LNC or LNC-CS were added to blood at 10% (v/v), significant levels of damage to the membrane were observed ($p < 0.05$). This result corroborates those of the hemolysis experiment described above.

Comparing the differences between the negatively and positively-charged (i.e., uncoated and coated) lipid-core nanocapsules when added to blood at a concentration of 10% (v/v), the highest LDH release was observed for LNC-CS. This result is consistent with other studies in which cationic particles or polymers caused greater adverse effects on blood cells and coagulation, without necessarily affecting all cellular function (Vermette and Meagher, 2003; Jones and Grainger, 2009). Moreover, the presence of a cationic polymer may not necessarily imply extensive membrane rupture and loss of hemoglobin components, but it is sufficient to cause an initial destabilization of the erythrocyte membrane and thus facilitate the release of the LDH enzyme from cells.

3.4.4. Platelets aggregation tests

The possibility of causing platelet aggregation by adding the lipid-core nanocapsule suspensions to the whole blood was studied by visualizing platelets in the blood samples by light microscopy and through the platelet count. To determine spontaneous aggregation PBS was used as the control. To this aim, peripheral blood smears were obtained using citrated whole blood incubated for 30 min in the presence of PBS (as the control) or in the presence of the nanocapsule suspensions [LNC or LNC-CS at 2 and 10% (v/v)] (Fig. 5). Erythrocytes, leucocytes and platelets were observed and the platelets are indicated on the microphotographs. The platelets were distributed evenly throughout in peripheral blood smears prepared with 2% (v/v) of nanocapsule suspensions in blood. Considering the light microscopy results, lipid-core nanocapsule suspensions added to blood at 2% (v/v) had little influence on the formation of platelet aggregates. On the other hand, small agglomerates could be visualized when lipid-core nanocapsule suspensions were added to blood at 10% (v/v) independently of their coating (LNC or LNC-CS).

As the platelets visualization by light microscopy have limited sensitivity in the evaluation of platelet aggregation, we performed additional analysis with a hematological counter. This method was carried out to evaluated platelet concentration and MPV (Fig. 6). The platelet concentration determined for whole blood and whole blood with PBS added at 2% (v/v) was maintained after adding LNC and LNC-CS suspensions to blood at 2% (v/v) ($p > 0.05$). MPV measurements corroborated these findings, since LNC or LNC-CS suspensions in the blood at 2% (v/v) did not show variations in this parameter ($p > 0.05$).

On the other hand, a decrease in the platelet concentration compared to the PBS solution was detected when LNC or LNC-CS suspensions were added to the blood at 10% (v/v) ($p < 0.05$). The results suggested that the lower number of platelets was a consequence of platelet aggregation since aggregates are counted as single particles. This is most evident when the MPV parameters were increased after adding LNC or LNC-CS suspensions to blood at 10% (v/v) ($p < 0.05$). The increase in the MPV associated with the lower number of platelets indicated significant platelet aggregation induced by both LNC and LNC-CS. In this case, the results indicated that the platelet aggregation was influenced by the increase in the specific surface area due to the addition of a higher volume fraction of the formulations in the blood samples and probably not to the chemical nature of the particle/water interface.

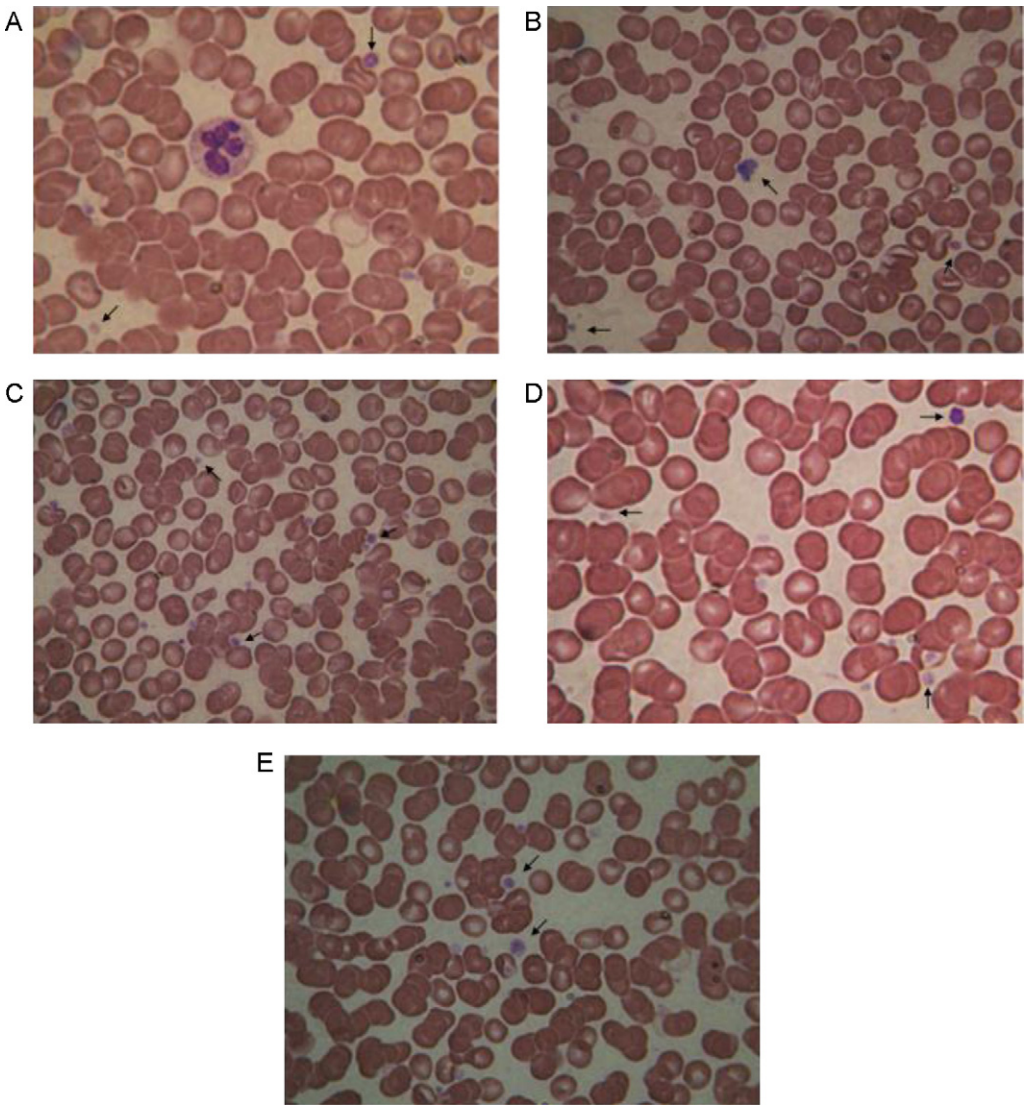

Fig. 5. Light microscopy: smears were made of human blood stimulated with (A) 2% LNC, (B) 10% LNC, (C) 2% LNC-CS, (D) 10% LNC-CS and (E) PBS as the control. Arrows indicate the presence of platelets. Images photographed at magnification of 1000×.

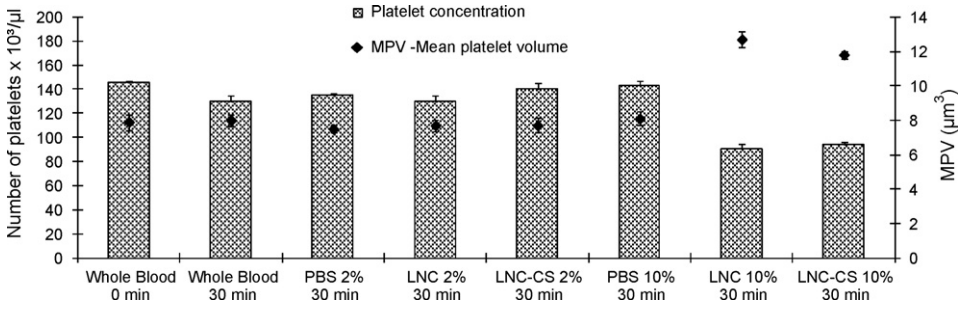

Fig. 6. Number of platelets and mean platelet volume (MPV) levels after adding the LNC or LNC-CS suspensions to citrated whole blood at 2% and 10% (v/v). All bars represent mean ± SD ($n = 3$).

4. Conclusions

Modified lipid-core nanocapsules were effectively obtained with negatively-charged (polysorbate 80-lecithin) and positively-charged (chitosan) surfaces. The hemocompatibility study carried out with the negatively and positively-charged lipid-core nanocapsule suspensions (LNC and LNC-CS) investigated at two different concentrations in human blood (2 and 10%, v/v) showed very promising results indicating good potential for their use in parenteral administration. Hence, regarding the activated partial thromboplastin time, neither of the suspensions when added to plasma at 2% (v/v) influenced the clotting time.

Furthermore, LNC and LNC-CS suspensions added to blood at 2% (v/v) showed no significant hemolysis or platelet aggregates

indicating their compatibility independently of the chemical nature of their surface. Hemolysis and platelet aggregation observed for the suspensions added to blood at high concentration (10%, v/v) indicated that the specific surface area of the colloids influenced the results more than the chemical nature of the particle/water interface. Taking all data obtained into account we can infer that these lipid-core nanocapsules are potential systems for intravenous administration representing an innovative nanotechnological platform.

Acknowledgments

EAB thanks CAPES/Brazil for his fellowship. The authors thank FAPERGS (PqG), CNPq/FAPERGS (PRONEX and PRONEM), INCT-IF/CNPq, Rede Nanobiotecnologia CAPES and CNPq/Brasilia/Brazil for financial support. The authors are grateful to the Clinical Laboratory at UFRGS, especially to MSc. Ana Lúcia Antunes.

References

Aktas, Y., Yemisci, M., Andrieux, K., Gursoy, R.N., Alonso, M.J., Fernandez-Megia, E., Novoa-Carballal, R., Quinoa, E., Riguera, R., Sargon, M.F., Celik, H.H., Demir, A.S., Hincal, A.A., Dalkara, T., Capan, Y., Couvreur, P., 2005. Development and brain delivery of chitosan-PEG nanoparticles functionalized with the monoclonal antibody OX26. Bioconjugate Chem. 16, 1503–1511.

Alves, M.P., Scarrone, A.L., Santos, M., Pohlmann, A.R., Guterres, S.S., 2007. Human skin penetration and distribution of nimesulide from hydrophilic gels containing nanocarriers. Int. J. Pharm. 341, 215–220.

Baldrick, P., 2010. The safety of chitosan as a pharmaceutical excipient. Regul. Toxicol. Pharm. 56, 290–299.

Bernardi, A., Zilberstein, A., Jager, E., Campos, M.M., Morrone, F.B., Calixto, J.B., Pohlmann, A.R., Guterres, S.S., Battastini, A.M.O., 2009. Effects of indomethacin-loaded nanocapsules in experimental models of inflammation in rats. Br. J. Pharmacol. 158, 1104–1111.

Brazil. ANVISA – Agência Nacional de Vigilância Sanitária. Resolution RDC no. 57, 2010 December 16. Retrieved from http://bvsms.saude.gov.br/bvs/saudelegis/anvisa/2010/res0057_16_12_2010.html.

Byrne, J.D., Betancourt, T., Brannon-Peppas, L., 2008. Active targeting schemes for nanoparticle systems in cancer therapeutics. Adv. Drug Deliv. Rev. 60, 1615–1626.

Cai, G.Q., Jiang, H.L., Chen, Z.J., Tu, K.H., Wang, L.Q., Zhu, K.J., 2009. Synthesis, characterization and self-assemble behavior of chitosan-O-poly(epsilon-caprolactone). Eur. Polym. J. 45, 1674–1680.

Cattani, V.B., Fiel, L.A., Jager, A., Jager, E., Colome, L.M., Uchoa, F., Stefani, V., Dalla Costa, T., Guterres, S.S., Pohlmann, A.R., 2010. Lipid-core nanocapsules restrained the indomethacin ethyl ester hydrolysis in the gastrointestinal lumen and wall acting as mucoadhesive reservoirs. Eur. J. Pharm. Sci. 39, 116–124.

Celia, C., Trapasso, E., Cosco, D., Paolino, D., Fresta, M., 2009. Turbiscan Lab (R) Expert analysis of the stability of ethosomes (R) and ultradeformable liposomes containing a bilayer fluidizing agent. Colloids Surf. B 72, 155–160.

Cenni, E., Granchi, D., Avnet, S., Fotia, C., Salerno, M., Micieli, D., Sarpietro, M.G., Pignatello, R., Castelli, F., Baldini, N., 2008. Biocompatibility of poly(D,L-lactide-co-glycolide) nanoparticles conjugated with alendronate. Biomaterials 29, 1400–1411.

Cruz, L., Soares, L.U., Dalla Costa, T., Mezzalira, G., da Silveira, N.P., Guterres, S.S., Pohlmann, A.R., 2006. Diffusion and mathematical modeling of release profiles from nanocarriers. Int. J. Pharm. 313, 198–205.

Cui, Z.R., Mumper, R.J., 2001. Chitosan-based nanoparticles for topical genetic immunization. J. Control. Release 75, 409–419.

Dobrovolskaia, M.A., Patri, A.K., Zheng, J.W., Clogston, J.D., Ayub, N., Aggarwal, P., Neun, B.W., Hall, J.B., McNeil, S.E., 2009. Interaction of colloidal gold nanoparticles with human blood: effects on particle size and analysis of plasma protein binding profiles. Nanomedicine: NBM 5, 106–117.

Fessi, H., Puisieux, F., Devissaguet, J.P., Ammoury, N., Benita, S., 1989. Nanocapsule formation by interfacial polymer deposition following solvent displacement. Int. J. Pharm. 55, R1–R4.

Filipe, V., Hawe, A., Jiskoot, W., 2010. Critical evaluation of Nanoparticle Tracking Analysis (NTA) by NanoSight for the measurement of nanoparticles and protein aggregates. Pharm. Res. 27, 796–810.

Frozza, R.L., Bernardi, A., Paese, K., Hoppe, J.B., da Silva, T., Battastini, A.M.O., Pohlmann, A.R., Guterres, S.S., Salbego, C., 2010. Characterization of trans-resveratrol-loaded lipid-core nanocapsules and tissue distribution studies in rats. J. Biomed. Nanotechnol. 6, 694–703.

Gallego-Urrea, J.A., Tuoriniemi, J., Pallander, T., Hassellov, M., 2009. Measurements of nanoparticle number concentrations and size distributions in contrasting aquatic environments using nanoparticle tracking analysis. Environ. Chem. 7, 67–81.

Hogman, C.F., Hedlund, K., Sahlestrom, Y., 1981. Red-Cell preservation in protein-poor media. Protection against in vitro hemolysis. Vox Sang. 41, 274–281.

Huynh, N.T., Passirani, C., Saulnier, P., Benoit, J.P., 2009. Lipid nanocapsules: a new platform for nanomedicine. Int. J. Pharm. 379, 201–209.

Jager, A., Stefani, V., Guterres, S.S., Pohlmann, A.R., 2007. Physico-chemical characterization of nanocapsule polymeric wall using fluorescent benzazole probes. Int. J. Pharm. 338, 297–305.

Jager, E., Venturini, C.G., Poletto, F.S., Colome, L.M., Pohlmann, J.P.U., Bernardi, A., Battastini, A.M.O., Guterres, S.S., Pohlmann, A.R., 2009. Sustained release from lipid-core nanocapsules by varying the core viscosity and the particle surface area. J. Biomed. Nanotechnol. 5, 130–140.

Jakubowicz, J., 2008. Particle analysis and properties of mechanically alloyed $Nd_{16}Fe_{76-x}Ti_xB_8$. Superlattices Microstruct. 43, 315–323.

Jones, C.F., Grainger, D.W., 2009. In vitro assessments of nanomaterial toxicity. Adv. Drug Deliv. Rev. 61, 438–456.

Jones, M.N., 1999. Surfactants in membrane solubilisation. Int. J. Pharm. 177, 137–159.

Koziara, J.M., Oh, J.J., Akers, W.S., Ferraris, S.P., Mumper, R.J., 2005. Blood compatibility of cetyl alcohol/polysorbate-based nanoparticles. Pharm. Res. 22, 1821–1828.

Letchford, K., Liggins, R., Wasan, K.M., Burt, H., 2009. In vitro human plasma distribution of nanoparticulate paclitaxel is dependent on the physicochemical properties of poly(ethylene glycol)-block-poly(caprolactone) nanoparticles. Eur. J. Pharm. Biopharm. 71, 196–206.

Mayer, A., Vadon, M., Rinner, B., Novak, A., Wintersteiger, R., Frohlich, E., 2009. The role of nanoparticle size in hemocompatibility. Toxicology 258, 139–147.

Mengual, O., Meunier, G., Cayre, I., Puech, K., Snabre, P., 1999. TURBISCAN MA 2000: multiple light scattering measurement for concentrated emulsion and suspension instability analysis. Talanta 50, 445–456.

Michanetzis, G.P.A.K., Missirlis, Y.F., Antimisiaris, S.G., 2008. Haemocompatibility of nanosized drug delivery systems: has it been adequately considered? J. Biomed. Nanotechnol. 4, 218–233.

Mosqueira, V.C.F., Legrand, P., Pinto-Alphandary, H., Puisieux, F., Barratt, G., 2000. Poly(D,L-lactide) nanocapsules prepared by a solvent displacement process: influence of the composition on physicochemical and structural properties. J. Pharm. Sci. 89, 614–626.

Nafee, N., Schneider, M., Schaefer, U.F., Lehr, C.M., 2009. Relevance of the colloidal stability of chitosan/PLGA nanoparticles on their cytotoxicity profile. Int. J. Pharm. 381, 130–139.

Oyarzun-Ampuero, F.A., Garcia-Fuentes, M., Torres, D., Alonso, M.J., 2010. Chitosan-coated lipid nanocarriers for therapeutic applications. J. Drug Deliv. Sci. Tech. 20, 259–265.

Prego, C., Paolicelli, P., Diaz, B., Vicente, S., Sanchez, A., Gonzalez-Fernandez, A., Jose Alonso, M., 2010. Chitosan-based nanoparticles for improving immunization against hepatitis B infection. Vaccine 28, 2607–2614.

Skotak, M., Leonov, A.P., Larsen, G., Noriega, S., Subramanian, A., 2008. Biocompatible and biodegradable ultrafine fibrillar scaffold materials for tissue engineering by facile grafting of L-lactide onto chitosan. Biomacromolecules 9, 1902–1908.

Vermette, P., Meagher, L., 2003. Interactions of phospholipid- and poly(ethylene glycol)-modified surfaces with biological systems: relation to physico-chemical properties and mechanisms. Colloids Surf. B 28, 153–198.

von Ahsen, N., Lewczuk, P., Schutz, E., Oellerich, M., Ehrenreich, H., 2000. Prothrombin activity and concentration in healthy subjects with and without the prothrombin G20210A mutation. Thromb. Res. 99, 549–556.

Wang, B., He, C., Tang, C., Yin, C., 2011. Effects of hydrophobic and hydrophilic modifications on gene delivery of amphiphilic chitosan based nanocarriers. Biomaterials 32, 4630–4638.

Xu, D., Wu, K., Zhang, Q.H., Hu, H.Y., Xi, K., Chen, Q.M., Yu, X.H., Chen, J.N., Jia, X.D., 2010. Synthesis and biocompatibility of anionic polyurethane nanoparticles coated with adsorbed chitosan. Polymer 51, 1926–1933.

Zern, B.J., Chu, H.H., Osunkoya, A.O., Gao, J., Wang, Y.D.A., 2011. Biocompatible arginine-based polycation. Adv. Funct. Mater. 21, 434–440.